

Strength failure behavior of granite containing two holes under Brazilian test

Yan-Hua Huang ^{1a}, Sheng-Qi Yang ^{*1} and Chun-Shun Zhang ²

¹ State Key Laboratory for Geomechanics and Deep Underground Engineering, School of Mechanics and Civil Engineering, China University of Mining and Technology, Xuzhou 221116, P.R. China

² Department of Civil Engineering, Monash University, Clayton, VIC 3800, Australia

(Received May 20, 2016, Revised November 18, 2016, Accepted January 16, 2017)

Abstract. A series of Brazilian tests under diameter compression for disc specimens was carried out to investigate the strength and failure behavior by using acoustic emission (AE) and photography monitoring technique. On the basis of experimental results, load-displacement curves, AE counts, real-time crack evolution process, failure modes and strength property of granite specimens containing two pre-existing holes were analyzed in detail. Two typical types of load-displacement curves are identified, i.e., sudden instability (type I) and progressive failure (type II). In accordance with the two types of load-displacement curves, the AE events also have different responses. The present experiments on disc specimens containing two pre-existing holes under Brazilian test reveal four distinct failure modes, including diametrical splitting failure mode (mode I), one crack coalescence failure mode (mode II), two crack coalescences failure mode (mode III) and no crack coalescence failure mode (mode IV). Compared with intact granite specimen, the disc specimen containing two holes fails with lower strength, which is closely related to the bridge angle. The failure strength of pre-holed specimen first decreases and then increases with the bridge angle. Finally, a preliminary interpretation was proposed to explain the strength evolution law of granite specimen containing two holes based on the microscopic observation of fracture plane.

Keywords: granite; two pre-existing holes; disc specimen; tensile strength; crack coalescence

1. Introduction

Holes and fissures, as pre-existing flaws, often present in the nature rock mass. Compared with the intact rock, the pre-existing holes and fissures significantly weaken the mechanical properties and affect the cracking behavior of rock material. Different geometries of pre-existing holes and fissures have different responses on the mechanical behavior. In recent years, the influences of pre-fissures on the strength and deformation behavior have been widely studied (Cao *et al.* 2016, Duriez *et al.* 2016, Huang *et al.* 2016, Lee and Jeon 2011, Park and Bobet 2010, Yin *et al.* 2014, Zhou *et al.* 2015, Haeri *et al.* 2014 and 2015c). Moreover, some experimental and numerical results of rock containing pre-existing holes also have been reported by Zhao *et al.* (2014), Wong *et al.* (2006), Tang *et al.* (2005), Yin *et al.* (2015), Liu *et al.* (2015), Lin *et al.* (2015), Yang (2015), Zhou *et al.* (2016), Haeri (2015), Haeri *et al.* (2015b). However, most of the above investigations

*Corresponding author, Professor, E-mail: yangsqi@hotmail.com

^a Ph.D. Student, E-mail: huangyh1219@163.com

were limited to compression tests.

As a kind of typical heterogeneous material, the tensile strength of rock is much lower than the compressive strength. Generally, the tensile strength of rock only performs 1/12~1/8 of the compressive value. The tensile strength of rocks thence is an essential mechanical parameter in the design and construction of rock engineering. Brazilian test under diameter compression has been a suggested method to measure the tensile strength of rock (Bieniawski and Hawkes 1978) due to its simple procedure and convenient preparation. The strength failure and crack propagation behavior of rock containing pre-existing holes under tension have been tested and simulated. A series of Brazilian tests under diametrical compression were carried out by Mellor and Hawkes (1971) to investigate the crack initiation, propagation behavior of rock with a central hole. Haeri *et al.* (2015a) took the radius of holes and interaction of multiple holes into account in their experimental and modeling study. To investigate the effect of a tensile stress gradient on crack initiation and propagation, Steen *et al.* (2005) conducted some Brazilian tests for disc rock sample with an eccentric hole. Their simulations by using the boundary element code DIGS further confirmed the laboratory results. RFPA3D code was also adopted to analyze the strength characteristic and crack distribution of rock disc with a central or eccentric hole by Wang *et al.* (2014).

In underground engineering, such as mines, tunnels and hydropower stations, rock mass stability is influenced by the excavations. Study on the strength and failure behavior of pre-holed rock is very significant to predict unstable failure of rock mass engineering. In previous studies, the rock specimen was often machined with pre-existing holes to investigate the mechanical and cracking behaviors, which is easy to control the loading/boundary conditions and also can monitor more data during the failure process of specimen (Wang *et al.* 2013). The pre-existing holes aim to simulate the underground openings (Fakhimi *et al.* 2002), because the circular openings are cross-sectional structure in underground engineering. Rock mass instability after excavation were often occurred due to the strong stress interactions between holes (Lin *et al.* 2013). However, up to now, no laboratory experiments have been reported on granite disc specimens containing two pre-existing holes with different bridge angles. In addition, in the previous experimental investigations for disc specimens containing pre-holes, the acoustic emission (AE) characteristics have not been fully investigated. Hence, in this research, disc specimens containing two pre-existing holes under Brazilian test were carried out by using a rock material testing system. Furthermore, photographic monitoring and AE monitoring techniques were both used to construct the relationship between load level and real-time crack propagation process for granite specimen containing two holes. Finally, the microscopic observation of fracture plane was obtained to reveal the meso-mechanism of strength and cracking behavior under tension. Hopefully, this laboratory experimental study could provide more fundamental knowledge of fracture behavior of rock, for example the cracks interaction between two tunnels when excavation.

2. Tested material and testing procedure

2.1 Granite material and sample preparation

The granite from Quanzhou city in the Fujian province of China, was used as the tested rock material for this study. Based on X-ray diffraction (XRD) analysis and thin section (see Fig. 1(a)), the mineral components of the tested granite are primarily feldspar, quartz, amphibole, etc. The granite is a medium-grained heterogeneous material (see Fig. 1(b)), which has an average unit

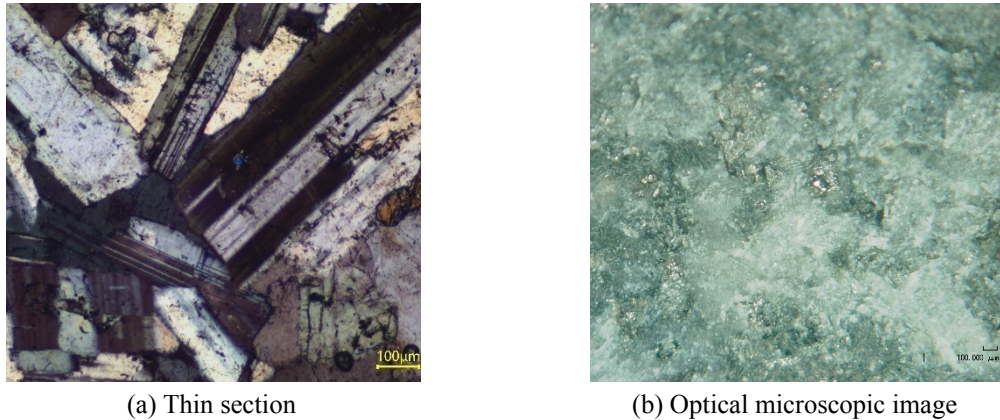


Fig. 1 Microscopic structure of tested granite

weight of about 2730 kg/m^3 .

Two holes distribution was designed to investigate the strength and failure behavior under diameter compression, as shown in Fig. 2. In Fig. 2(a), R is the disc specimen radius, t is the thickness of disc specimen, r is the hole radius, l is the distance of the centers of two holes, and α is the angle between line l and the loading direction. The granite block was first cut into rectangular shape with a thickness of about 30 mm, and the rock surfaces were polished smooth to reduce the frictional effects. Then, both the internal holes and disc specimens were made using high pressure water jet cutting. All the machine process was controlled automatically by a computer, thus we can obtain the accurate designed dimensions. In this research, the specimen size was fixed at $\Phi 60 \text{ mm}$ ($2R$) \times 30 mm (t), with the thickness to diameter ratio of 0.5, which was satisfied the dimensional requirements (Bieniawski and Hawkes 1978). The r and l were designed to 4.0 mm and 19.4 mm, respectively. In order to investigate the effect of hole geometry on the

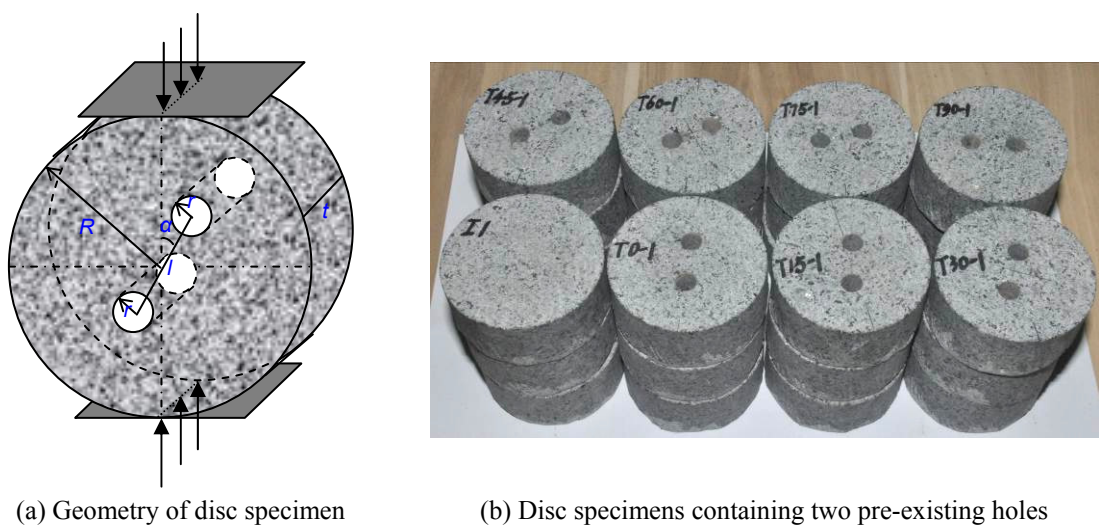


Fig. 2 Granite specimens containing two holes used for this study

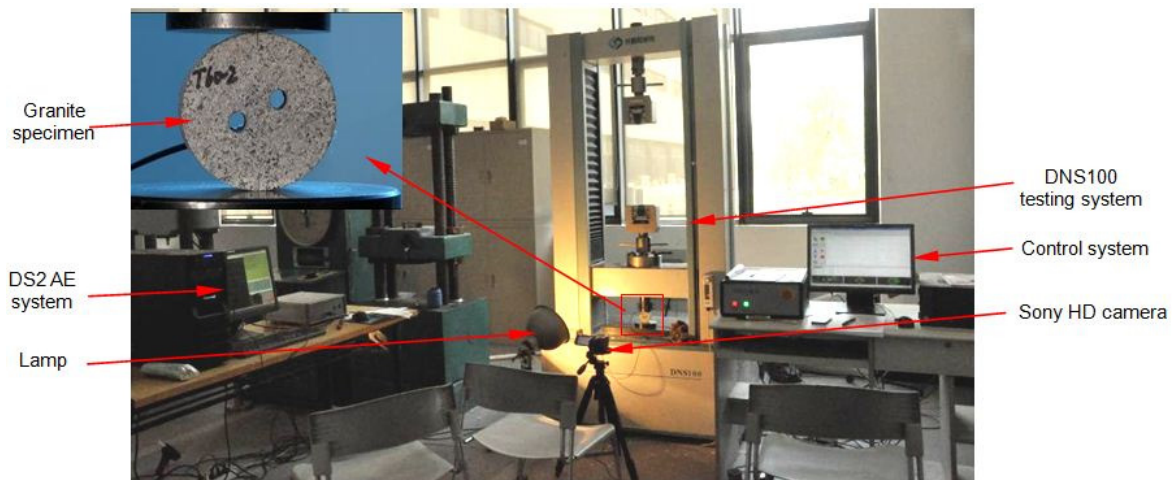


Fig. 3 The rock mechanics testing and AE system for Brazilian test

strength, AE and failure behaviors of granite specimens, the bridge angle α varied from 0° to 90° with an interval of 15° in this study. The tested intact and pre-holed disc specimens are present in Fig. 2(b).

2.2 Testing procedure

Fig. 3 shows the experiment setup for granite specimen under Brazilian test in this study. All the Brazilian tests were carried out on a DNS100 rock material testing system. Axial force was applied along the diameter direction of disc specimen under displacement controlled condition with a rate of 0.1 mm/min until the rock failure took place.

During the test, a DS2 full-information AE measuring system was adopted to record the real-time AE signals. At the same time, a Sony HDR-XR550E video camera was used to capture the whole fracture process. This is a continuous shooting triggering progress, which yields 25 frames per second to ensure clear cracks. As shown in Fig. 3, two AE sensors were stuck on the back face of granite specimen to avoid affecting the crack images catch on the front face.

3. Deformation and AE characteristics

3.1 Load-displacement curves

Fig. 4 shows the load-displacement curves of intact and pre-holed granite specimens under Brazilian test. For the intact specimen, as shown in Fig. 4(a), the upward concaved initial stage was clearly observed, due to the closure of some micro flaws. In the linear deformation stage, the load increased linearly with the displacement. Once the specimen was loaded to the peak value, the curve dropped abruptly and drastically, which resulted from the typical brittle response of the tested granite. Compared with the intact specimen, the peak value and slope of the curves of pre-holed specimens were lower, indicating that the pre-existing holes had a significant influence on strength and stiffness.

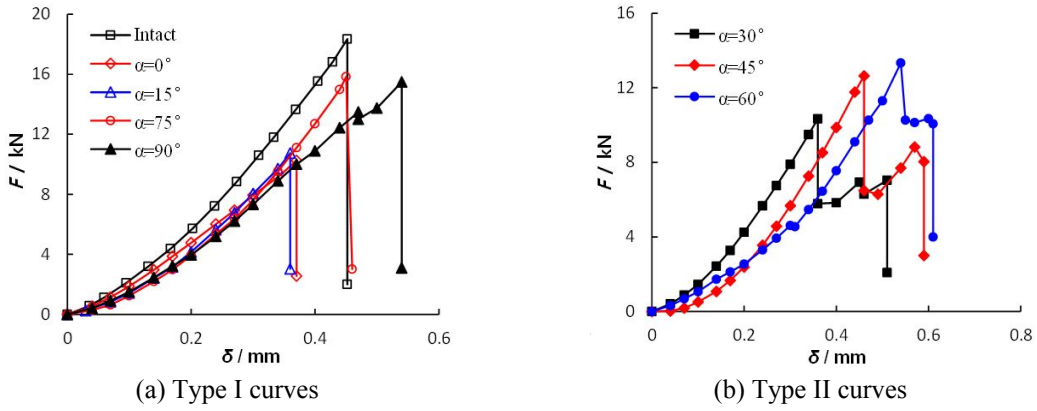


Fig. 4 Load-displacement curves of disc specimens under Brazilian test

As can be seen in Fig. 4, the pre-holed specimens with different bridge angles had different load-displacement responses, which can be divided into two categories: sudden instability (type I) and progressive failure (type II). The pre-holed specimens with bridge angles of 0°, 15°, 75° and 90°, had similar performance with the intact specimen. For type I curve as shown in Fig. 4(a), the failure happened suddenly at the peak load. However, from Fig. 4(b), the type II curve was quite different from type I curve. When pre-holed specimens with bridge angles of 30°, 45° and 60° were loaded to the peak value, these specimens would not fail abruptly. At the post-peak stage of type II curve, multiple load-drops were clearly observed, which resulted from the crack initiation and propagation.

3.3 AE characteristics

AE as an effective non-destructive testing method has been an important way to understand the mechanical properties and damage evolution of rock. Based on the full information recorded by DS2 AE measuring system, AE events were obtained to analyze the damage evolution during the process of crack initiation and propagation.

Figs. 5-6 show the relationship between load and AE counts of intact and pre-holed granite specimens. For intact specimen shown in Fig. 5(a), there was almost no AE count before peak load, which means that no macro crack emanates at this stage. At the peak load, an obvious AE count can be observed. At the moment, a huge failure sonic was heard due to the rapid failure.

For the other type I curves, as shown in Figs. 5(b), (c), (c) and (d), the AE curves have the similar evolution characteristic as the intact one. As can be seen from these figures, the maximum AE counts occur at the peak load. It needs to be noted that a relatively small but obvious AE count corresponding to a load drop in the load-time curve occurs at the initial and linear stages. However, we did not observe any macro crack initiation on the specimen surface, implying that these AE counts might be related to the internal damage.

For the type II curves, as shown in Figs. 5(d), 6(a) and 6(b), the AE evolution characteristics in these specimens were different from the above type I curves. With the multiple load-drops at the post-peak stage, some huge AE counts were observed. However, the AE counts at the post-peak stage were less than those at the peak load, which implies that the fracture at peak value released the most energy.

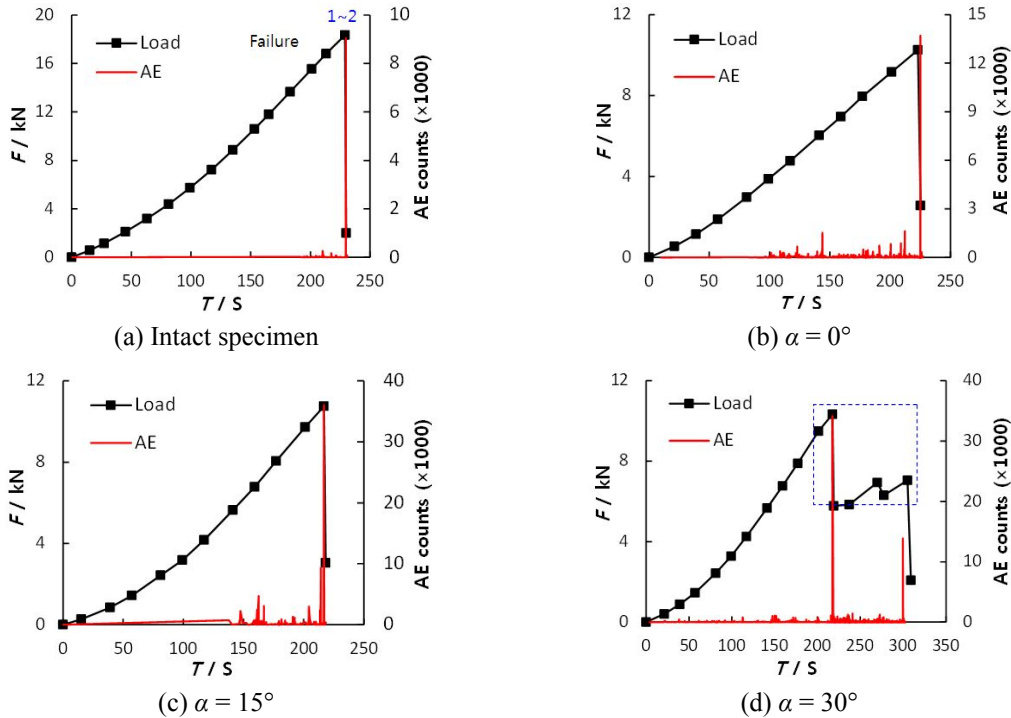


Fig. 5 AE counts of granite specimens during whole deformation for α smaller than or equal to 30°

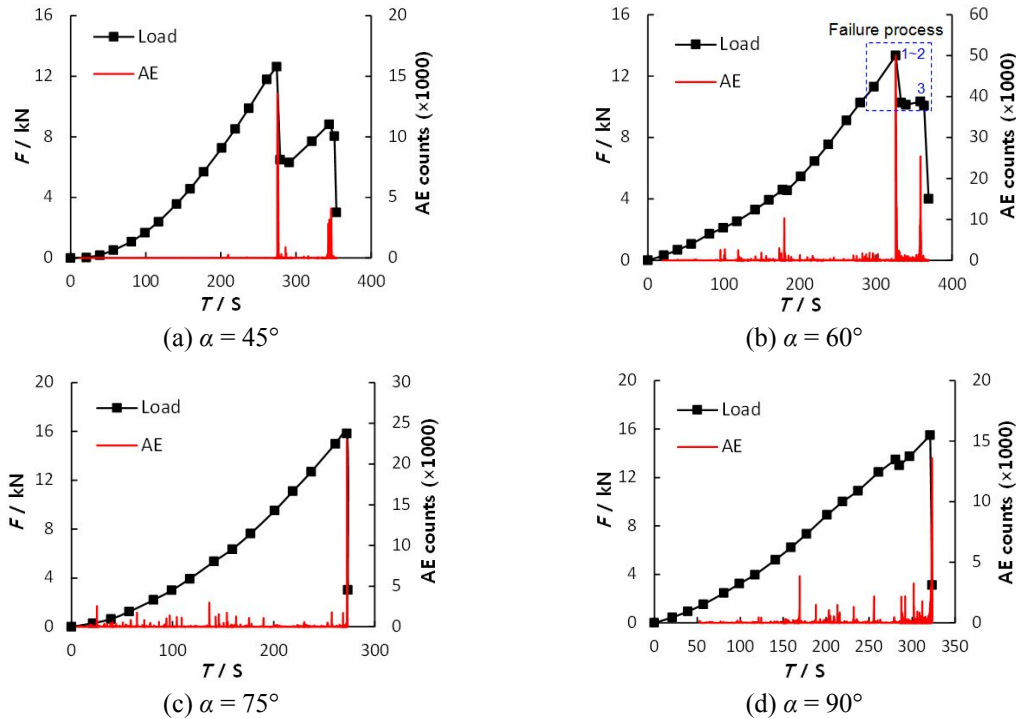


Fig. 6 AE counts of granite specimens during whole deformation process for α greater than 30°

4. Cracking behavior analysis

In accordance with the above analysis, we can conclude that the load-displacement curves and AE characteristics were closely related to the fracture process. On the basis of the fracture images recorded by a high definition camera during testing, the whole process of crack initiation, propagation and coalescence and ultimate failure was obtained.

4.1 Crack evolution process

Figs. 7-9 show the crack initiation, propagation and coalescence process of disc specimens under Brazilian test. Note that the denoted numbers in Figs. 7-9 correspond to the crack order as shown in Figs. 5-6.

Fig. 7 shows the fracture process of intact granite specimen under Brazilian test. From Fig. 7(b), some minor cracks are first initiated along the loading direction. From the local magnification, we can see that the growth paths of cracks are not smooth because of the resistance of the mineral grains. More and more minor cracks are initiated along the loading direction which also can be testified in the local magnification image. Finally, these minor cracks coalesce to form a main diametrical crack and then separate the whole disc specimen into two parts. The abrupt failure of intact disc specimen is conducted in only one (1) second.

Fig. 8 shows the crack propagation process of granite specimen containing two holes with bridge angle of 30° under Brazilian test. In Fig. 8, when the specimen is loaded to peak value (point 1), the first two cracks emanate from the top edge of the upper hole and the boundary the

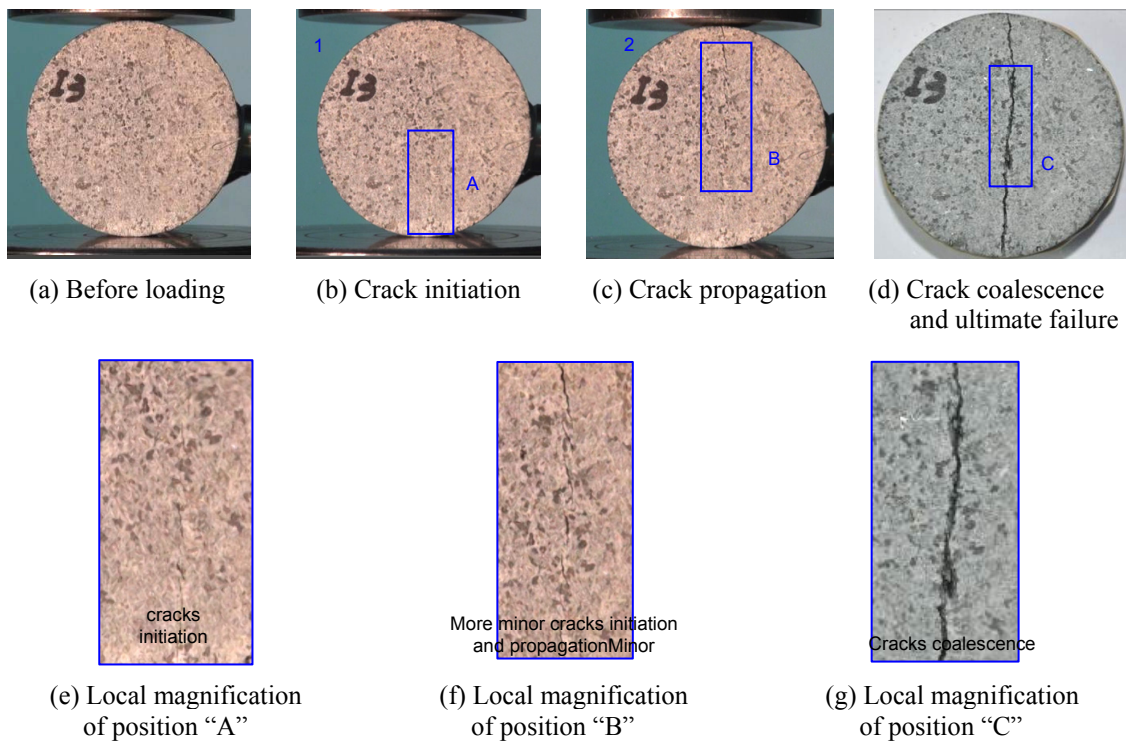


Fig. 7 Fracture process of intact disc specimen under Brazilian test

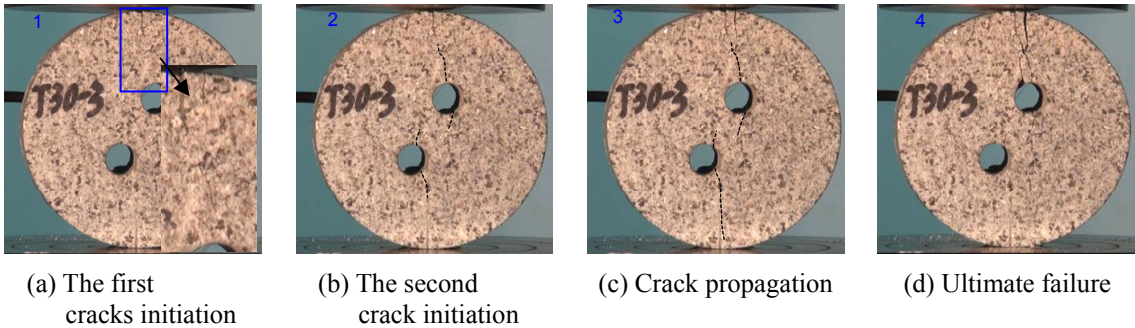


Fig. 8 Crack propagation process of granite specimen containing two holes under Brazilian test ($\alpha = 30^\circ$)

disc specimen, respectively. With the first crack initiation, the load drops to 55.7% of peak value. Afterwards, the force reloads to point 2. At the time, three cracks are observed around the two pre-existing holes. The continuous increasing the deformation leads the original cracks to quickly propagate and extend. Afterwards, when the specimen is loaded to point 4, a secondary crack is initiated from the top edge of the top hole and links the original cracks. At that moment, two coalescences between the two pre-existing holes occur due to the crack propagation. With these crack initiation and coalescence, ultimate brittle failure then occurs quickly and the specimen is separated into two dominant and several small parts. From the first crack initiation (point 1) to ultimate instability (point 4), the failure of granite specimen containing two holes is a progressive process and it lasts about 88 seconds.

Fig. 9 shows the crack propagation process of granite specimen containing two holes with bridge angle of 60° under Brazilian test. As can be seen in Fig. 9, when the specimen is loaded to peak value, a primary crack emanates from the top edge of the lower hole and grows upwards. Afterwards, another tensile crack is initiated from the bottom and right edge of the lower hole and propagates downwards. The two main cracks are initiated in one second. In the above processes, the load drops from peak value (13.34 kN) to 10.23 kN. After the load drop, the load increases slightly to point 3. At this time, a secondary crack is observed from the bottom boundary of disc specimen. However, the failure process from the first crack initiation (point 1) to ultimate instability (point 3) lasts about 70 seconds, which implies the failure is a progressive process.

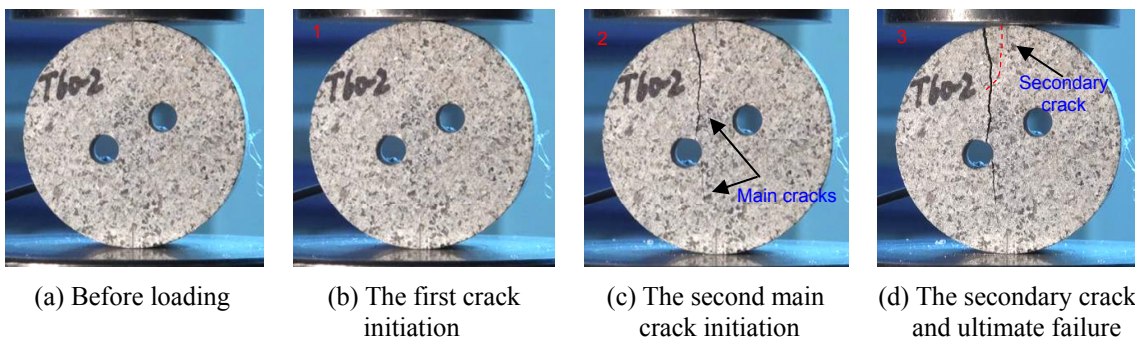


Fig. 9 Crack propagation process of granite specimen containing two holes under Brazilian test ($\alpha = 60^\circ$)

4.2 Macro failure modes

Fig. 10 shows the ultimate failure modes of disc specimens for different bridge angles under Brazilian test. The failure mode of intact disc specimen was also presented in Fig. 10. From Fig. 10, we can see that the failure pattern of disc specimen containing two pre-existing holes is dependent on the bridge angle. The patterns and characteristics of cracking behavior of disc specimens were summarized in Table 1. Four distinct failure modes were described in detail as follows

Mode I: Diametrical splitting failure-intact specimen, $\alpha = 75^\circ$ and $\alpha = 90^\circ$.

The intact disc specimen failed into two parts due to the main diametrical crack. Herein, this kind of failure mode was named as the diametrical splitting failure mode. The diametrical splitting mode was also observed in the pre-holed specimens with bridge angles of 75° and 90° . As can be seen from Fig. 10, in the pre-holed specimens with bridge angles of 75° and 90° , no crack was observed around the edges of the pre-existing holes. In other words, the pre-existing holes had no nearly any influence on the ultimate failure mode. In addition, the diametrical splitting failure mode corresponded to type I load-displacement curve.

Mode II: One crack coalescence failure - $\alpha = 0^\circ$ and $\alpha = 15^\circ$.

For pre-holed specimens with bridge angles of 0° and 15° , the macro failure modes were different from that of the above diametrical splitting failure mode. In these specimens, the main cracks were all initiated from the edges of the pre-existing holes and propagated along the loading direction. Moreover, one crack coalescence occurred between the two pre-existing holes and the disc specimens were separated into two parts. This mode corresponded to type I load-displacement curve. Herein, this kind of macro mode was named as one crack coalescence failure mode.

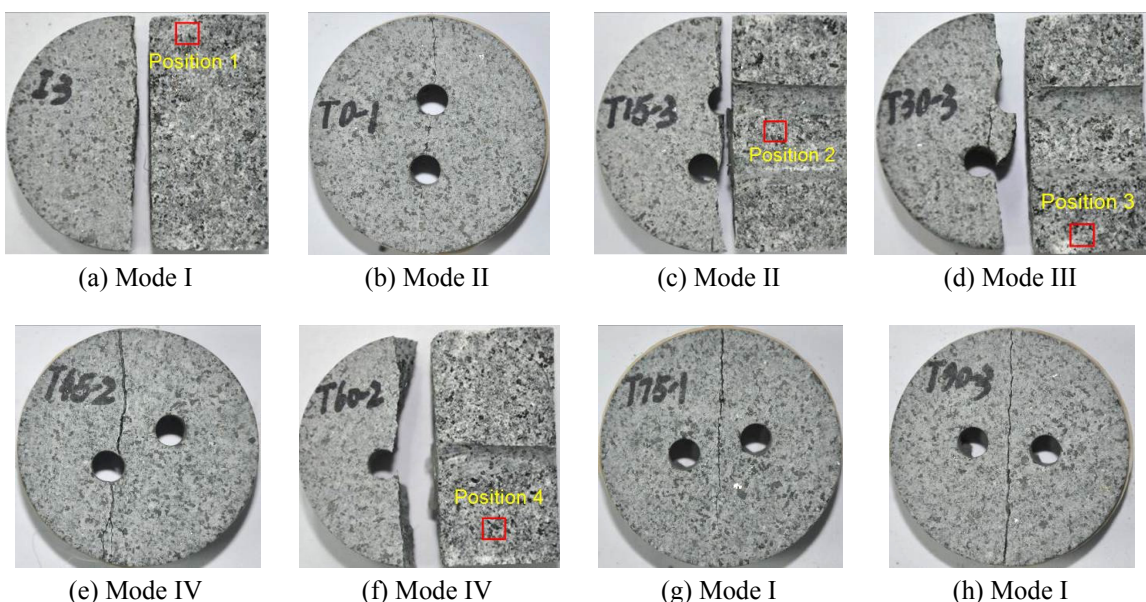
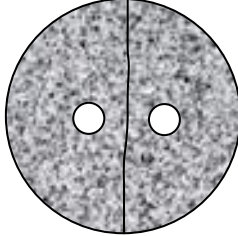
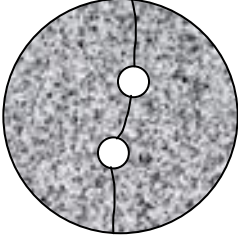
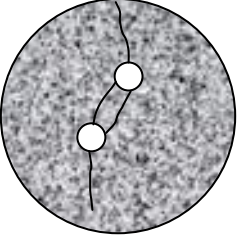
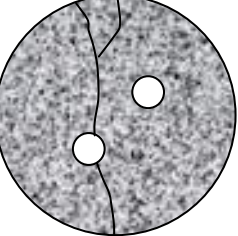


Fig. 10 Ultimate failure modes of granite specimens under Brazilian test

Table 1 Crack patterns and characteristics of the four failure modes under Brazilian test

	Mode I	Mode II	Mode III	Mode IV
Patterns				
Characteristics	<ul style="list-style-type: none"> Many minor cracks were first initiated and coalesced to form a diametrical crack along the diameter direction Specimen was separated into two parts Failure occurred in a second This mode corresponded to type I curve 	<ul style="list-style-type: none"> Tensile cracks were initiated from the edges of pre-holes One crack coalesced between the two holes Specimen was separated into two parts Failure occurred in a second This mode corresponded to type I curve 	<ul style="list-style-type: none"> Tensile cracks were initiated from the edges of pre-holes Two cracks coalesced between the two holes Specimen was divided into three dominant parts Failure was a progressive process This mode corresponded to type II curve 	<ul style="list-style-type: none"> Main cracks were first initiated from the edges of pre-holes No crack coalesced between the two holes Specimen was divided into two dominant parts Failure was a progressive process This mode corresponded to type II curve

Mode III: Two crack coalescences failure - $\alpha = 30^\circ$.

Compared with the diametrical splitting failure and one crack coalescence failure modes, the cracking mode of pre-holed specimen with bridge angle of 30° was obviously different as shown in Fig. 10. The failure mode of pre-holed specimen with bridge angle 30° was dependent on the pre-existing holes. Cracks initiation and propagation were clearly observed around the two pre-existing holes. Two crack coalescences occurred in the rock bridge area due to the crack growth and finally the specimen was divided into three parts. In this study, we named this failure pattern as two crack coalescences failure mode. This mode corresponded to type II load-displacement curve.

Mode IV: No crack coalescence failure - $\alpha = 45^\circ$ and 60°

The crack mode of pre-holed specimen with bridge angle of 45° was very similar to that of 60° . In these two specimens, the crack modes were different from those of other specimens. As can be seen from Fig. 10, the pre-holed specimens with bridge angle of 45° and 60° failed due to the primary cracks, which were initiated respectively from the top and bottom edges of the lower hole. In general, secondary cracks were initiated from the boundary of the disc specimen. The specimen was divided into two dominant parts and a small piece. This pattern, namely no crack coalescence failure mode, corresponded to load-displacement type II curve.

5. Strength property and discussion

In this study, the normalized failure load was defined as the failure load of the pre-holed disc specimen normalized by the average failure load of intact ones. The average failure load of intact disc specimens was about 18.5 kN.

The normalized failure loads of granite specimen containing two pre-existing holes under Brazilian tests were plotted in Fig. 11. From Fig. 11, it was clear that all the normalized failure loads were less than 1 because of the decrease effect of pre-existing holes on strength property. Moreover, the normalized failure loads were closely related to the bridge angle. The failure strength of pre-holed specimen first decreased then increased with increasing bridge angle. When the bridge angle increased from 0° to 15°, the average peak failure load of pre-holed specimen decreased from 10.8 kN to 9.8 kN, and the reduction extent was about 9.3%. When the bridge angle increased from 15° to 75°, the peak failure load of pre-holed specimen increased from 9.8 kN to 15.7 kN, and the increasing extent was about 60.2%, whereas the increasing extent was only 9.8% in the range of 75° to 90°, indicating that the effect of pre-holes on the strength was weakening.

In order to investigate the mechanism of failure strength evolution and cracking behavior of specimen containing two pre-existing holes, microscopic observations of fracture plane after failure were observed by a KH-3000VD three dimensional optical microscopy system. Figs.12-13 show the microscopic observations of fracture plane with different failure modes: mode I (G-I3[#]), mode II (G-T15-3[#]), mode III (G-T30-3[#]) and mode IV (G-T60-2[#]), respectively.

As can be seen in Fig. 12(a), the angularities of the mineral grains were clearly observed on the fracture plane of G-I3[#] specimen. Grains were broken under tension and some minor fractures were initiated, which also can be testified by the many minor cracks on the intact specimen surface (see Fig. 7). The behavior of grains broken may indicate that the meso-mechanism of this failure mode was transgranular fracture. In accordance with the crack pattern and characteristic of this mode (mode I in Table 1), the peak failure loads of failure mode I specimens, including intact specimen and pre-holed specimens with bridge angles of 75° and 90° were greater than that of other failure modes (see Fig. 11).

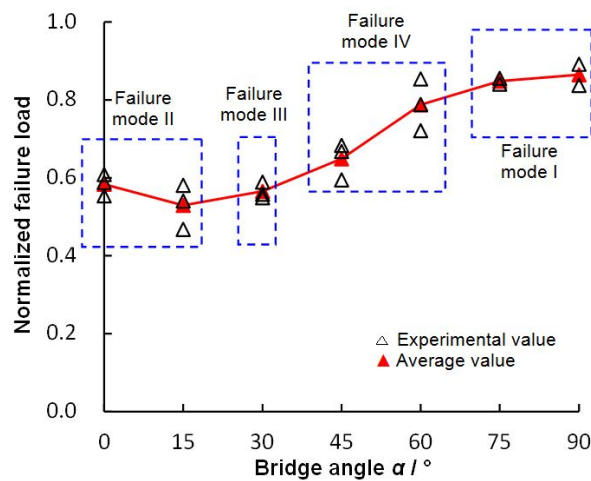
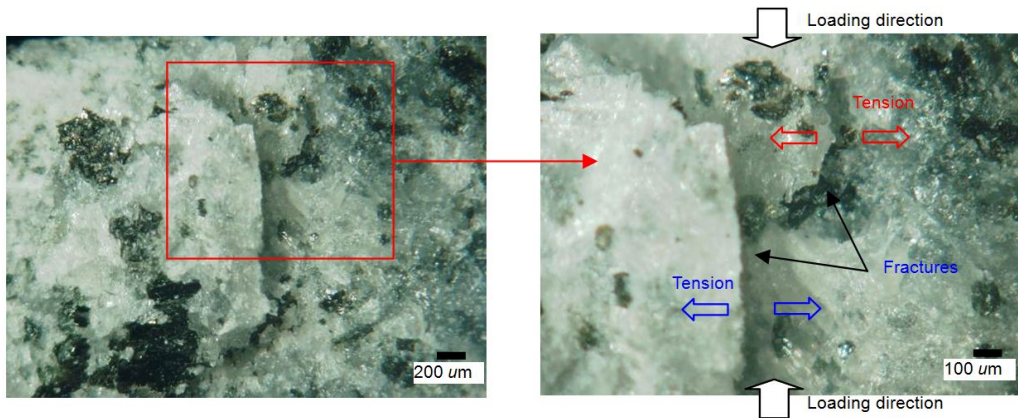


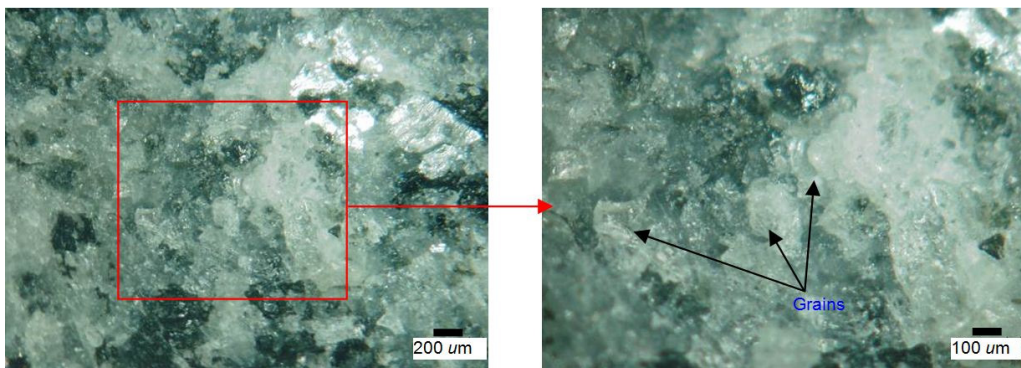
Fig. 11 Relation between normalized failure load and bridge angle under Brazilian test

From Fig. 12(b), the mineral grains were very smooth and no obvious angularities could be observed on the fracture plane of G-T15-3[#] specimen. Furthermore, the mineral grains kept relatively intact and no micro fractures appeared as shown in Fig. 12(b), which may imply this failure mode (mode II in Table 1) was under intergranular fracture mechanism. Therefore, the specimens with bridge angles of 0° and 15° born mainly by the bond between grains, leading to a lower strength (see Fig. 11). The micro-observation of pre-holed specimen with angle of 30° (see Fig. 13(a)) was similar to that of 15° and thus the strength of this failure mode (mode III in Table 1) was also relatively lower than other specimens.

From Fig. 13(b), some minor fractures also could be observed on the fracture plane of G-T60-2[#] specimen. Although the whole deformation of this failure mode was a progressive process, the observed fracture plane was an abrupt crack. The micro-observation of this failure mode (mode IV in Table 1) was similar to the intact specimen as shown in Fig. 12(a), whereas its fracture serious extent was less than intact specimen. Expect for the minor fracture, the other grains on the plane still kept relatively intact, which may mean that this failure mode was under mixed transgranular and intergranular fracture mechanism. Therefore, the strengths of mode IV specimens were relatively greater than those of mode II and mode III specimens, but were lower than those of mode I specimens.



(a) Local magnification of position 1 (see Fig. 10) corresponding to failure mode I



(b) Local magnification of position 2 (see Fig. 10) corresponding to failure mode II

Fig. 12 Typical microscopic observation of disc granite specimen after failure for mode I and II

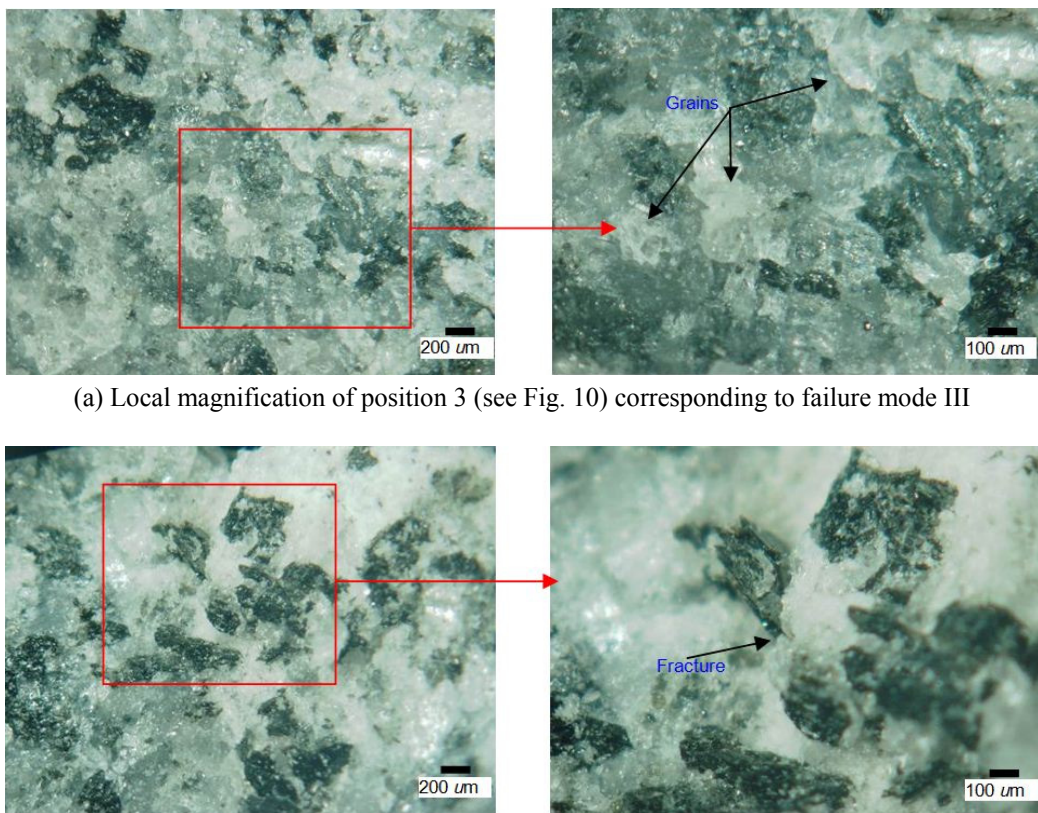


Fig. 13 Typical microscopic observation of disc granite specimen after failure for mode III and IV

6. Conclusions

- The tested granite specimen containing two pre-existing holes under Brazilian test has two different types of load-displacement curves results from the effect of bridge angles. Two typical types of load-displacement curves are identified, i.e., sudden instability (type I) and progressive failure (type II). In accordance with the two types of load-displacement curves, the AE counts also have different responses. For type I curve, the maximum AE counts are observed at the peak load, while for type II curve, some huge AE counts also can be observed at the post-peak stage.
- The failure mode of granite specimen containing two holes shows a significant dependence on the bridge angle. The present experiments on specimens containing two hole under Brazilian test reveal four distinct failure modes, i.e., diametrical splitting failure mode (mode I), one crack coalescence failure mode (mode II), two crack coalescences failure mode (mode III) and no crack coalescence failure mode (mode IV).
- The peak failure loads of granite specimen containing two pre-existing holes are all lower than that of intact specimen, and the reduction extent is distinctly related to the bridge angle. The failure strength of pre-holed specimen first decreases and then increases with the bridge angle. A preliminary interpretation of the strength evolution law of granite specimen

containing two holes is proposed based on the microscopic observation of fracture plane.

This investigation relied on photographic monitoring and AE technique to obtain the real-time crack coalescence process in the process of the whole deformation failure. The present study not only increases the understanding of pre-existing hole effect on the strength of granite, but also its effect on the cracking behavior. The experimental results on the fracture coalescence behavior of fractured rock can attribute to the development of fractured rock mechanics and increase the understanding of the unstable failure mechanism of rock engineering. However, due to the experimental limitations and the complexity of rock texture, further theoretical and numerical studies are necessary to better understand the strength failure behavior of rock containing pre-existing holes under tension.

Acknowledgments

This research was supported the Natural Science Foundation of Jiangsu Province for Distinguished Young Scholars (BK20150005), the Fundamental Research Funds for the Central Universities (2014XT03), the Innovation Project of Jiangsu Province (KYZZ16_0216). The authors would also like to express their sincere gratitude to the editors and two reviewers for their valuable comments, which have greatly improved this paper.

References

- Bieniawski, Z.T. and Hawkes, I. (1978), "Suggested methods for determining tensile strength of rock materials", *Int. J. Rock Mech. Min. Sci. Geomech. Abstr.*, **15**(1), 99-103.
- Cao, R.H., Cao, P., Fan, X., Xiong, X. and Lin, H. (2016), "An experimental and numerical study on mechanical behavior of ubiquitous-joint brittle rock-like specimens under uniaxial compression", *Rock Mech. Rock Eng.*, **49**(11), 4319-4338.
- Duriez, J., Scholtès, L. and Donzé, F.V. (2016), "Micromechanics of wing crack propagation for different flaw properties", *Eng. Fract. Mech.*, **153**, 378-398.
- Fakhimi, A., Carvalho, F., Ishida, T. and Labuz, J.F. (2002), "Simulation of failure around a circular opening in rock", *Int. J. Rock Mech. Min. Sci.*, **39**(2), 507-515.
- Haeri, H. (2015), "Propagation mechanism of neighboring cracks in rock-like cylindrical specimens under uniaxial compression", *J. Min. Sci.*, **51**(3), 487-496.
- Haeri, H., Shahriar, K., Marji, M.F. and Moarefvand, P. (2014), "Cracks coalescence mechanism and cracks propagation paths in rock-like specimens containing pre-existing random cracks under compression", *J. Cent. South Univ.*, **21**(6), 2404-2414.
- Haeri, H., Khaloo, A. and Marji, M.F. (2015a), "Fracture analyses of different pre-holed concrete specimens under compression", *Acta Mech. Sin.*, **31**(6), 855-870.
- Haeri, H., Marji, M.F., Shahriar, K. and Moarefvand, P. (2015b), "On the HDD analysis of micro crack initiation, propagation, and coalescence in brittle materials", *Arab. J. Geosci.*, **8**(5), 2841-2852.
- Haeri, H., Shahriar, K., Marji, M.F. and Moarefvand, P. (2015c), "A coupled numerical-experimental study of the breakage process of brittle substances", *Arab. J. Geosci.*, **8**(2), 809-825.
- Huang, Y.H., Yang, S.Q., Tian, W.L., Zeng, W. and Yu, L.Y. (2016), "An experimental study on fracture mechanical behavior of rock-like materials containing two unparallel fissures under uniaxial compression", *Acta Mech. Sin.*, **32**(3), 442-455.
- Lee, H. and Jeon, S. (2011), "An experimental and numerical study of fracture coalescence in pre-cracked specimens under uniaxial compression", *Int. J. Solids Struct.*, **48**(6), 979-999.

- Lin, P., Zhou, Y., Liu, H. and Wang, C. (2013), "Reinforcement design and stability analysis for large-span tailrace bifurcated tunnels with irregular geometry", *Tunn. Undergr. Space Technol.*, **38**, 189-204.
- Lin, P., Wong, R.H.C. and Tang, C.A. (2015), "Experimental study of coalescence mechanisms and failure under uniaxial compression of granite containing multiple holes", *Int. J. Rock Mech. Min. Sci.*, **77**, 313-327.
- Liu, J.P., Li, Y.H., Xu, S.D., Xu, S., Jin, C.Y. and Liu, Z.S. (2015), "Moment tensor analysis of acoustic emission for cracking mechanisms in rock with a pre-cut circular hole under uniaxial compression", *Eng. Fract. Mech.*, **135**, 206-218.
- Mellor, M. and Hawkes, I. (1971), "Mesurment of tensile strength by diametral compression of disc and annuli", *Eng. Geo.*, **5**(3), 173-225.
- Park, C.H. and Bobet, A. (2010), "Crack initiation, propagation and coalescence from frictional flaws in uniaxial compression", *Eng. Fract. Mech.*, **77**(14), 2727-2748.
- Steen, B.V.D., Vervoort, A. and Napier, J.A.L. (2005), "Observed and simulated fracture pattern in diametrically loaded discs of rock material", *Int. J. Fract.*, **131**(1), 35-52.
- Tang, C.A., Wong, R.H.C., Chau, K.T. and Lin, P. (2005), "Modeling of compression-induced splitting failure in heterogeneous brittle porous solids", *Eng. Fract. Mech.*, **72**(4), 597-615.
- Wang, S.Y., Sun, L., Yang, C., Yang, S.Q. and Tang, C.A. (2013), "Numerical study on static and dynamic fracture evolution around rock cavities", *J. Rock Mech. Geotech. Eng.*, **5**(4), 262-276.
- Wang, S.Y., Sloan, S.W. and Tang, C.A. (2014), "Three-dimensional numerical investigations of the failure mechanism of a rock disc with a central or eccentric hole", *Rock Mech. Rock Eng.*, **47**(6), 2117-2137.
- Wong, R.H.C., Lin, P. and Tang, C.A. (2006), "Experimental and numerical study on splitting failure of brittle solids containing single pore under uniaxial compression", *Mech. Mater.*, **38**(1), 142-159.
- Yang, S.Q. (2015), "An experimental study on fracture coalescence characteristics of brittle sandstone specimens combined various flaws", *Geomech. Eng., Int. J.*, **8**(4), 541-557.
- Yin, P., Wong, R.H.C. and Chau, K.T. (2014), "Coalescence of two parallel pre-existing surface cracks in granite", *Int. J. Rock Mech. Min. Sci.*, **68**, 66-84.
- Yin, Q., Jing, H.W. and Ma, G.W. (2015), "Experimental study on mechanical properties of sandstone specimens containing a single hole after high-temperature exposure", *Géotech. Lett.*, **5**(1), 43-48.
- Zhao, X., Zhang, H. and Zhu, W. (2014), "Fracture evolution around pre-existing cylindrical cavities in brittle rocks under uniaxial compression", *Trans. Nonferrous Met. Soc. China*, **24**(3), 806-815.
- Zhou, X.P., Bi, J. and Qian, Q.H. (2015), "Numerical simulation of crack growth and coalescence in rock-like materials containing multiple pre-existing flaws", *Rock Mech. Rock Eng.*, **48**(3), 1097-1114.
- Zhou, S., Zhu, H., Yan, Z., Ju, J.W. and Zhang, L. (2016), "A micromechanical study of the breakage mechanism of microcapsules in concrete using PFC2D", *Constr. Build. Mater.*, **115**, 452-463.